SUPPLEMENTARY DATA

RNA-seq was performed in the Illumina HiSeq2000 platform. Sequencing reads were first quality checked with FastQC (http://www.bioinformatics.babraham.ac.uk/projects/fastqc/), subsequently aligned to mm10 using Tophat (version tophat-2.0.9). Aligned reads were then qualified using Cuffdiff (Version 2.1.1), which also performs statistical tests between tested conditions. Genes with low expression, defined by FPKM<0.1 in both tested conditions, were removed.

Complete list of RBP was downloaded from http://rbpdb.ccbr.utoronto.ca/help.php.. A RBP was considered significantly differentially expressed if (i) q-value<0.05 and (ii) more than 1.5 fold change between tested conditions.

RIP-seq analysis

RNA-seq analysis was performed as described above to obtain FPKM values for each gene. Genes with FPKM<1 in the RNA-seq from brown adipocytes were considered as undetectable in cells and were excluded. Genes with FPKM <5 in both IgG and anti-Ybx2 RIP-seq were regarded as unbound by Ybx2 and IgG and therefore also excluded. 5227 and 5883 genes passed these filters in WAT and BAT RIP-seq data for downstream analysis. The gene expression ratios between anti-Ybx2 and IgG were calculated as an indicator for the enrichment of each transcript by Ybx2 RIP. Because low FPKM values will introduce large noises to the ratios between anti-Ybx2 and IgG, RIP-seq data were adjusted by adding 0.5 FPKM on all genes before the ratios between anti-Ybx2 and IgG were derived.

SUPPLEMENTARY DATA

Supplementary Figure S1.(A) Western blots to detect the Ucp1 change in cultured primary brown adipocytes (day 5) where AKAP1 and RBPMS2 were knocked down by retroviral shRNA. (B, C) Metabolic flux curves from cultured brown adipocytes (Day 5) where AKAP1 and RBPMS2 were knocked down by retroviral shRNA. Oxygen consumption rates (OCR) are normalized by protein concentration. n=8. *p<0.05, one-way ANOVA.

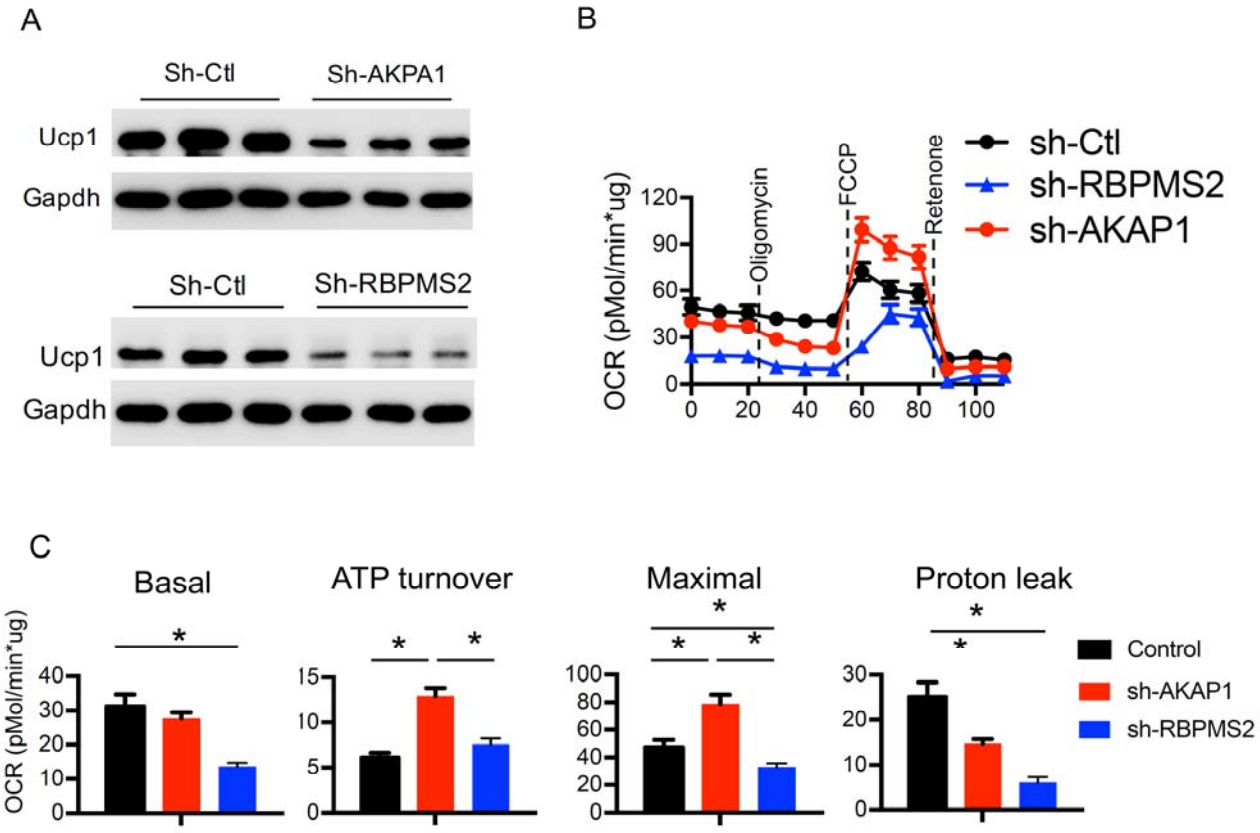

SUPPLEMENTARY DATA

Supplementary Figure S2. (A-D) Real-time PCR to examine the knockdown efficiency and marker expression in brown adipocytes expressing shRNAs targeting (A, B) Grsf1 and (C,D) Larp4. n=3. Error bars are mean ± SEM, *p<0.05, student's t test.
(E-G) Real-time PCR to measure the (E) knockdown efficiency, (F) pan-adipogenic markers and (G) BAT-selective markers in cultured primary white adipocytes (Day 5) that were infected by retroviral shRNAs targeting Ybx2. n=3. Error bars are mean ± SEM, *p<0.05, student's t test.
(H-K) Primary brown preadipocytes were infected by retroviral shRNAs (pMKO vector) targeting different regions of Ybx2 mRNA, followed by induction of differentiation for 5 days. (H) Oil-Red O staining (top) and TAG quantification (bottom) were used to assess lipid accumulation. Real-time PCR was performed to examine the (I) knockdown efficiency, (J) pan-adipogenic markers and (K) BAT-selective markers. (L) Similar to I-K, but in primary white adipocyte culture. n=4. Error bars are mean ± SEM, *p<0.05. one-way ANOVA

SUPPLEMENTARY DATA

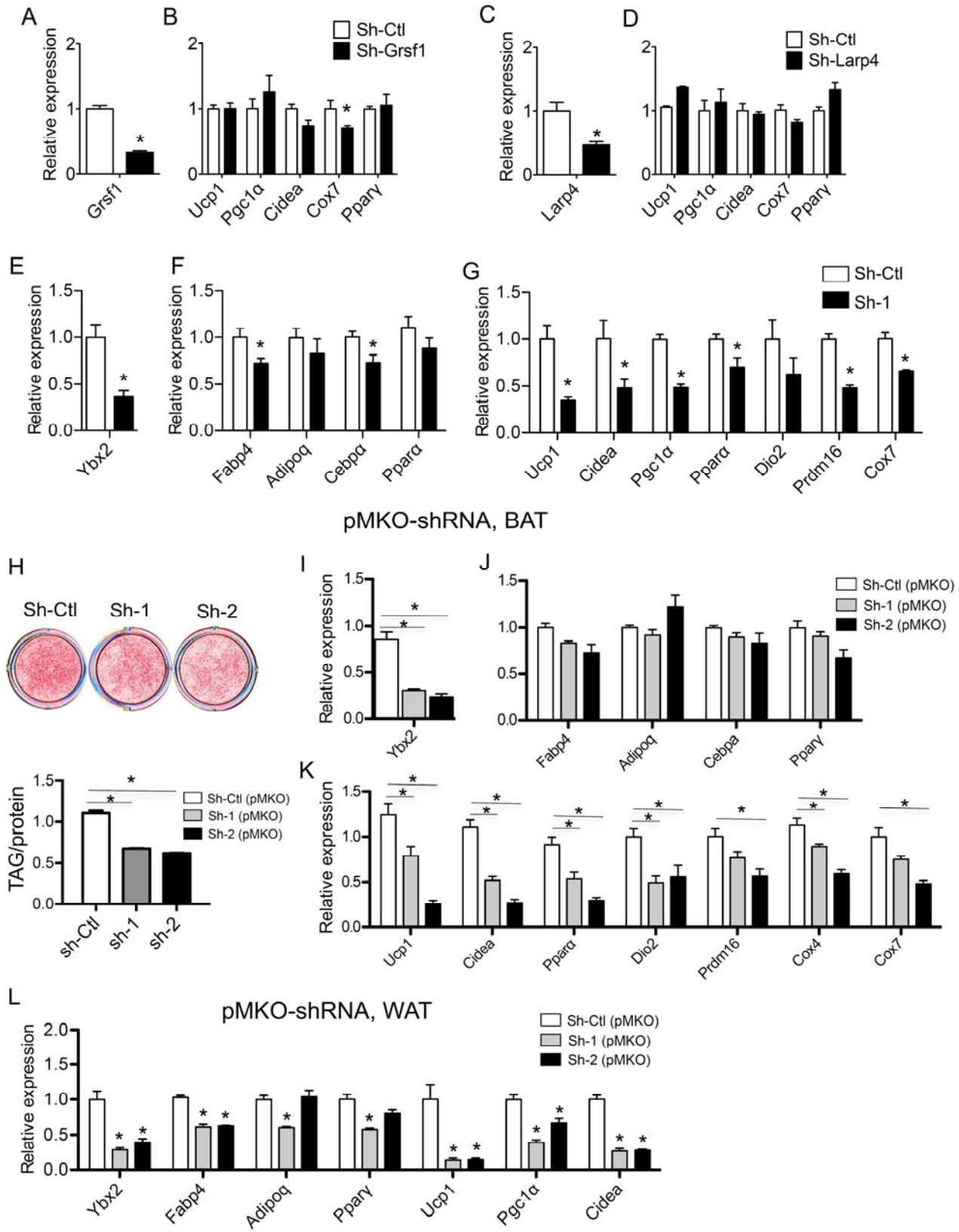

SUPPLEMENTARY DATA

Supplementary Figure S3. (A) Fat and (B) lean mass of male mice measured by EchoMRI. (C, D) Organ weight of iWAT and eWAT in WT and KO male mice at 9 weeks old. n≥6. Error bars are mean ± SEM, *p<0.05, student's t test.
(E) Real-time PCR of pan-abiogenic markers and (F) BAT-selective markers in WT and KO BAT. n≥7.
(G) Real-time PCR of marker expression in iWAT. n≥6. Error bars are mean ± SEM, *p<0.05, student's t test.
(H) Blood glucose levels during glucose tolerance test (n=5) and insulin tolerance test (n=10), 16 weeks old male animals. Error bars are mean ± SEM, *p<0.05, student's t test.

SUPPLEMENTARY DATA

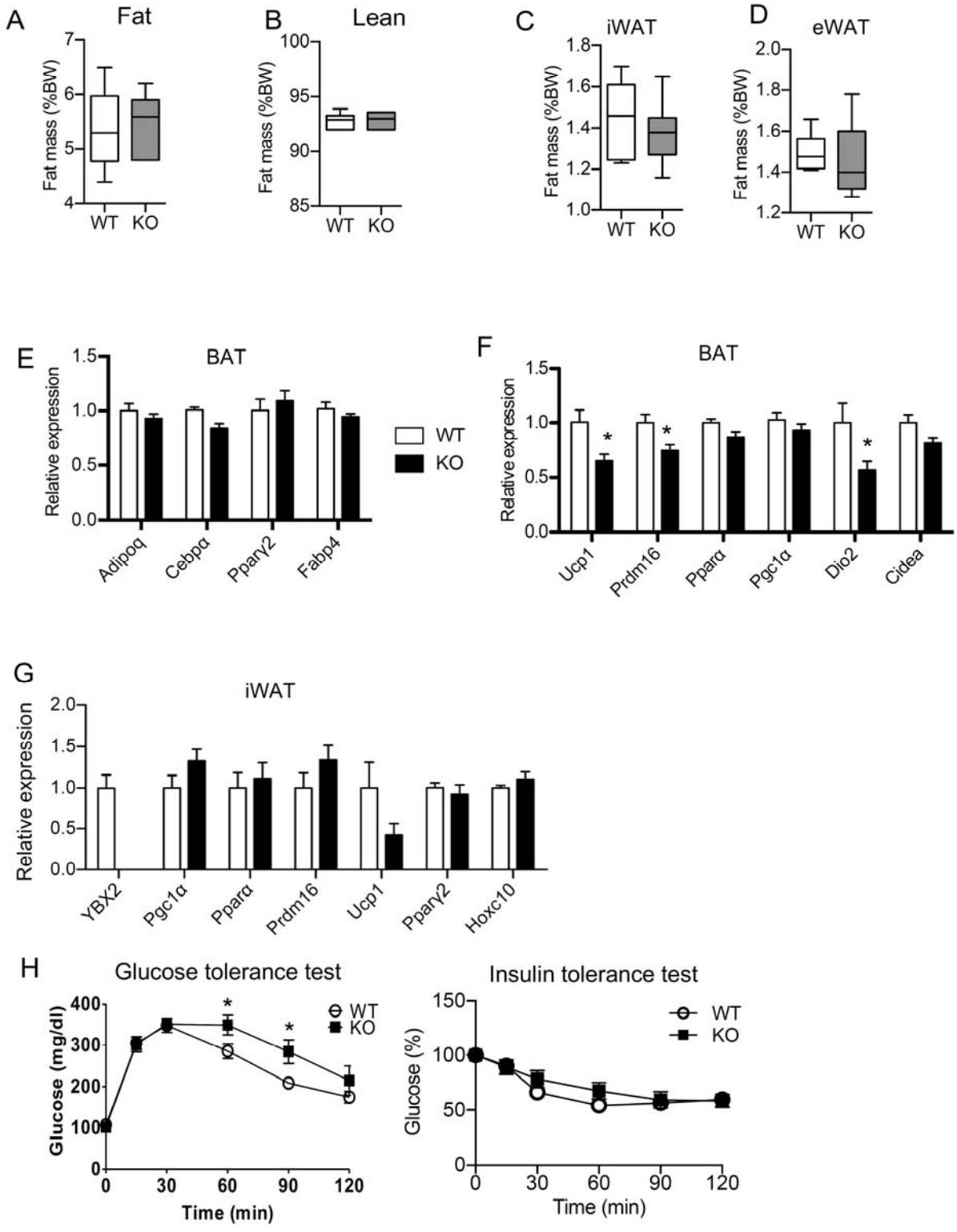

SUPPLEMENTARY DATA

Supplementary Figure S4. (A-C) primary brown preadipocytes were isolated from WT BAT and KO BAT *for in vitro* culture and differentiation for 5 days. Real-time PCR was used to confirm the (A) knockdown efficiency (B) pan-adipogenic markers (C) BAT-selective markers. n=3, Error bars are mean ± SEM, *p<0.05. Student's t test. (D) Genes were pre-ranked by their relative expression between KO and WT, followed by GSEA analysis.

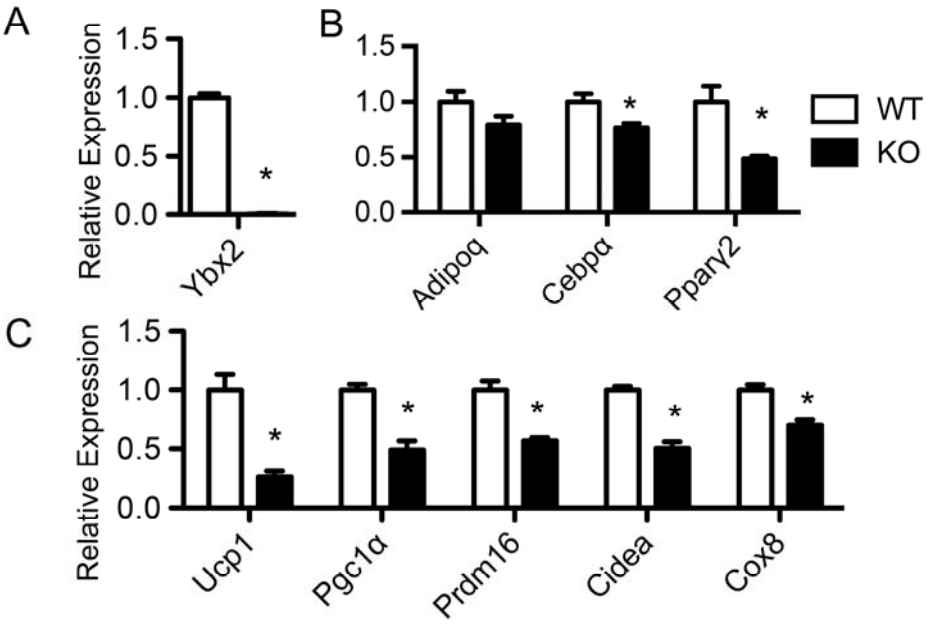

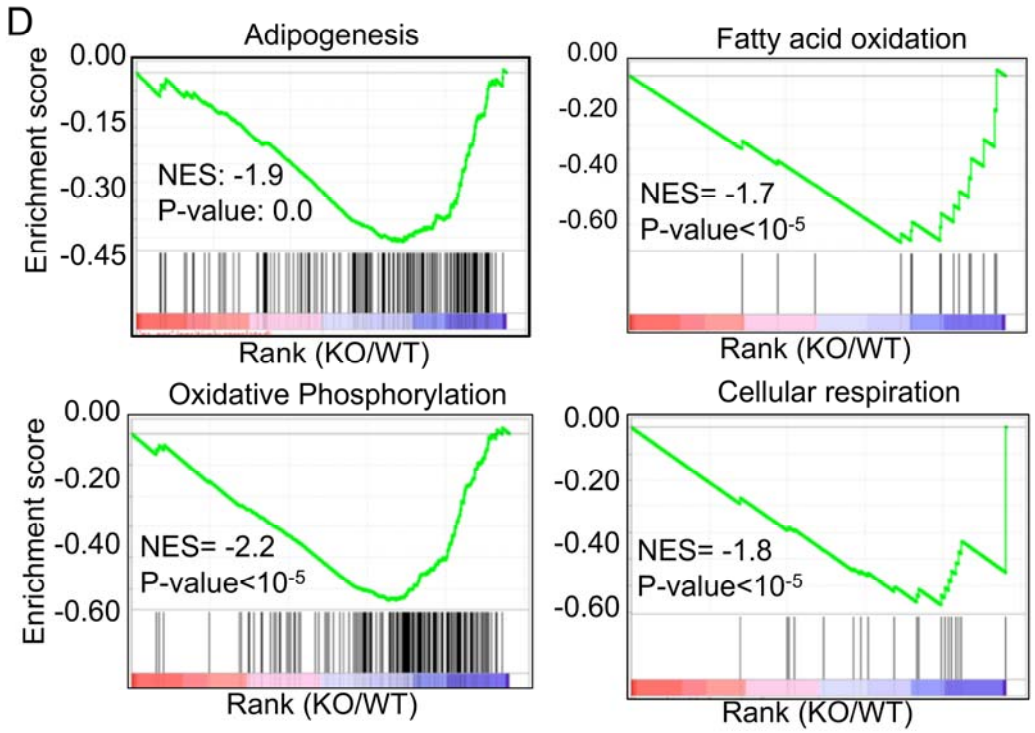

SUPPLEMENTARY DATA

Supplementary Figure S5. (A) The OCRs of WT and KO BAT were measured with Oroboros respirometry after housing 8-9 weeks old animals at 4°C for 6 hours. n=6, Error bars are mean ± SEM, *p<0.05. Student's t test (B) Lipolysis assay to assess the lipolysis rate of WT and KO BAT isolated from animals exposed to acute cold temperature. n=6. (C) 8-9 weeks old Ybx2 KO and WT male mice were fasted for 6 hours at RT or 4°C. Insulin (1 U per kg body weight) were injected into these animals. Mice were then sacrificed after 5 mins injection. Brown adipose tissue were collected. Western Blot was performed to detect protein levels of P-AKT and AKT in BAT. (D) Real-time PCR to examine BAT-selective markers in iWAT after acute cold exposure. n≥9, *p<0.05, Student's t-test.

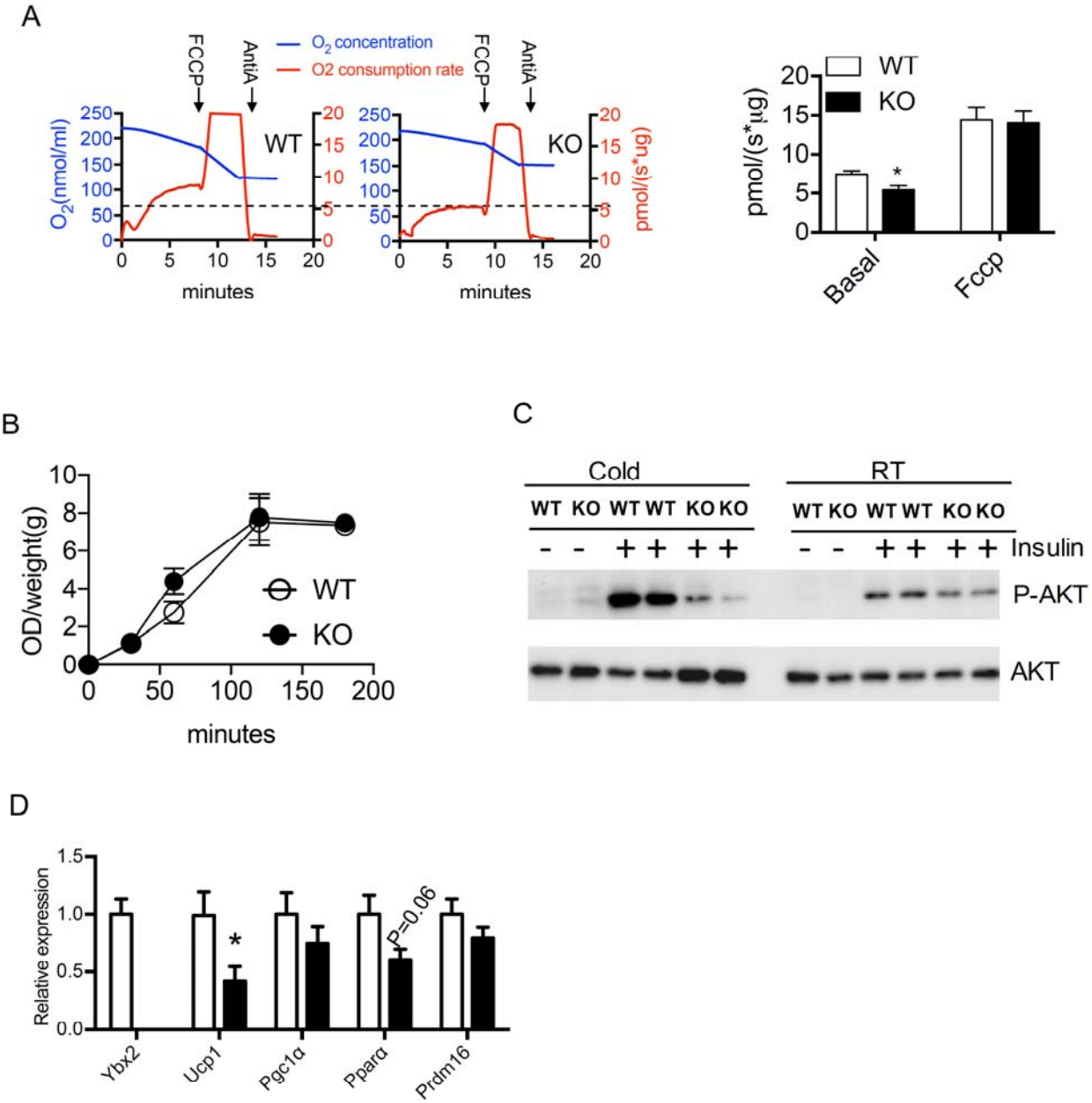

SUPPLEMENTARY DATA

Supplementary Figure S6. (A) FPKM of thermogenic markers in WT and KO BAT at room temperature and after cold treatment. (B) The fold changes (FC) of gene expression upon cold exposure were calculated for WT and KO BAT. The genes with more than 2 fold difference in FC were plotted in heatmap, and the color code represents the column mean-centered FC. (C) Pathway analysis was performed using DAVID Tools.

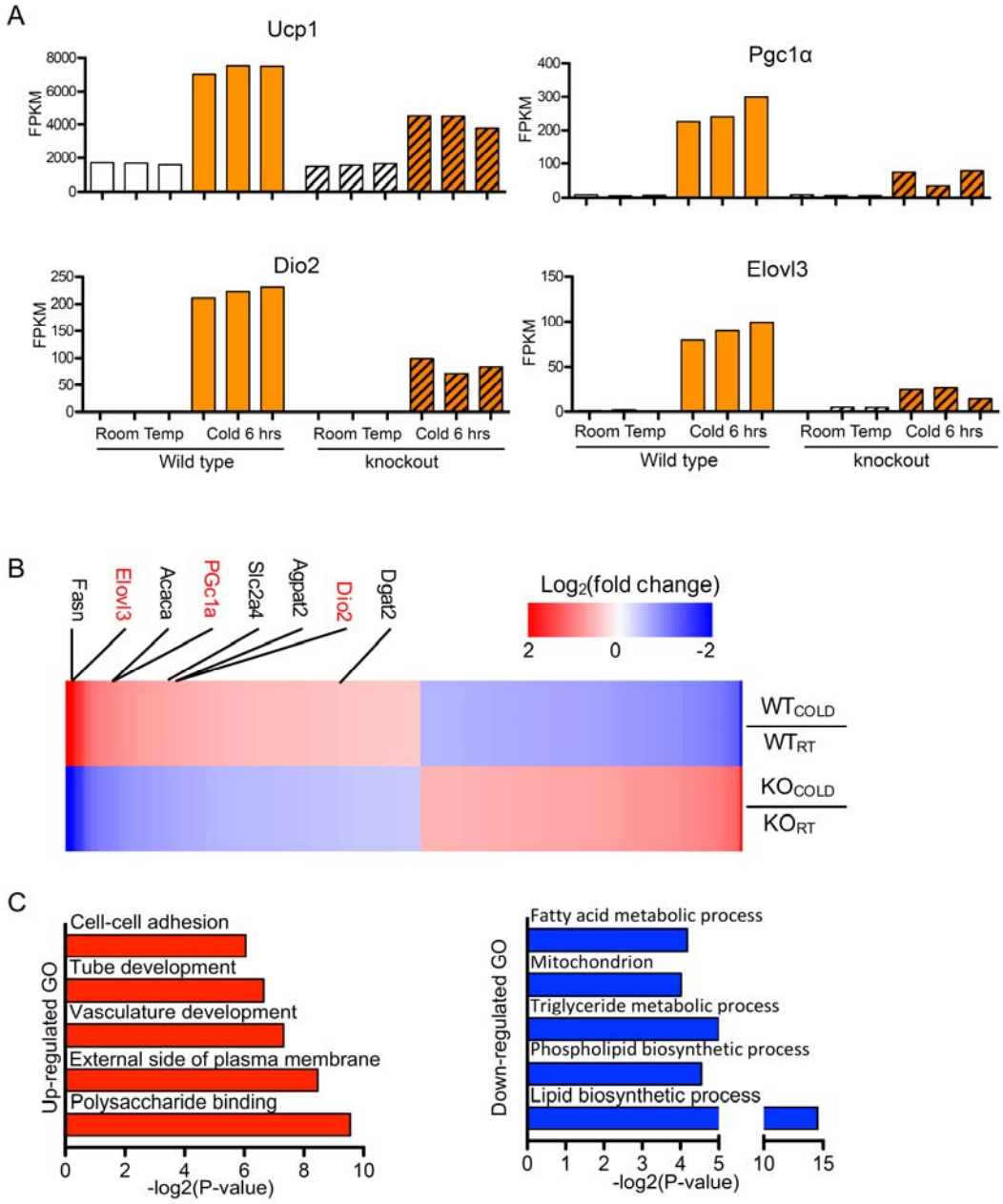

SUPPLEMENTARY DATA

Supplementary Figure S7. (A) Body weight, (B) BAT mass (C) iWAT mass of female mice at 8-9 weeks after 6-hours cold challenge. n=6 (D) Real-time PCR to examine BAT-selective and (E) lipogenesis markers in BAT from female mice upon cold treatment (4°C,6 hours). 9 weeks old, n=6. Error bars are mean ± SEM, *p<0.05, student's t test.

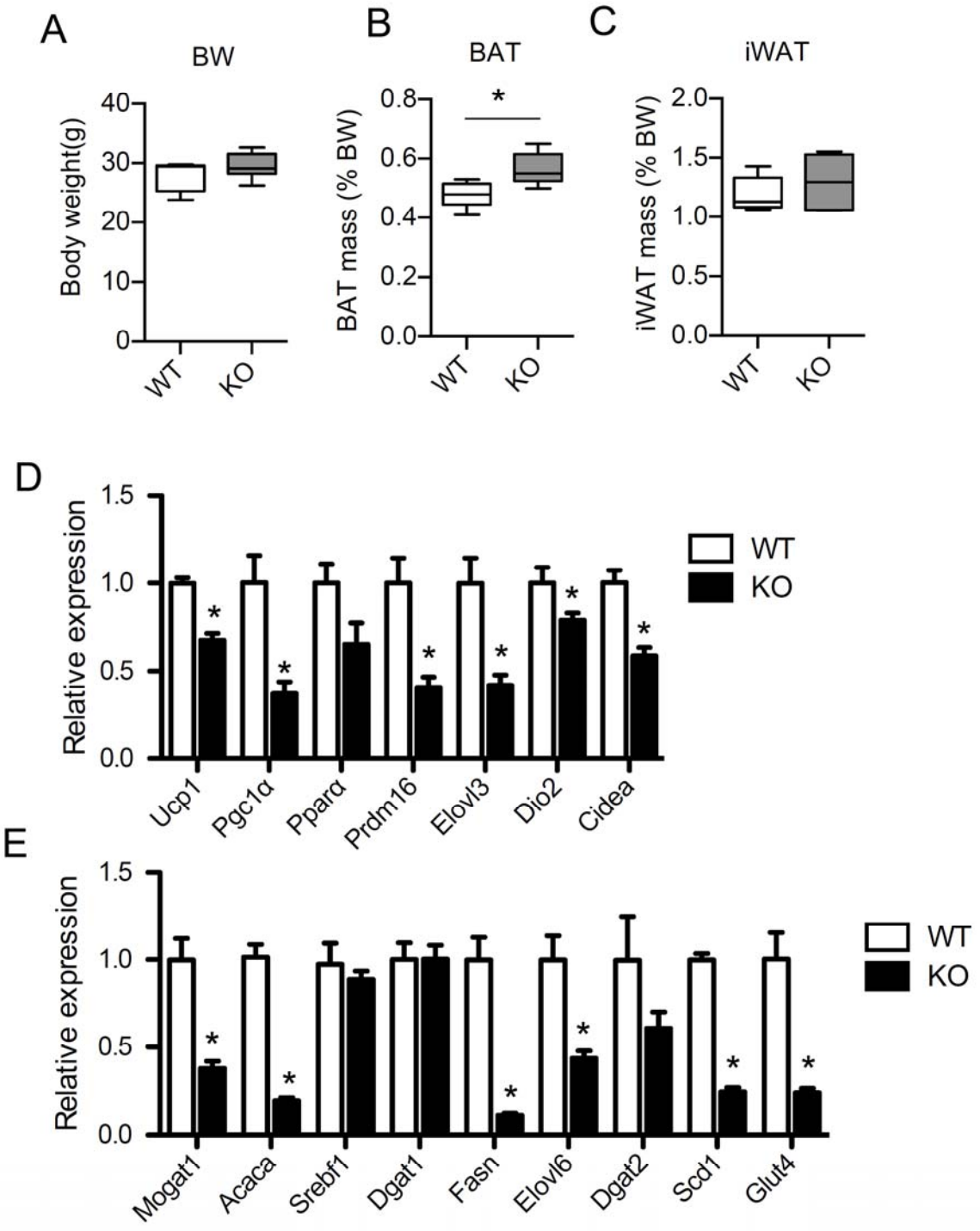

SUPPLEMENTARY DATA

Supplementary Figure S8. (A) Diagram of the RIP-seq experiments. (B) RIP-PCR analysis to detect the Ybx2-Pgc1a mRNA interaction in differentiated brown adipocytes which was treated with NE for 6 hours in the presence of Actinomycin D. (C) 293 cells were transfected with a reporter plasmid (psi-Check2) harboring a ~2kb WT Pgc1a 3'UTR or a mutant plasmid without the Ybx2 binding sites in the presence or absence of YBX2. Actinomycin D was added to stop transcription, and RNAs were harvested at the indicated time points (X-axis) after transcription inhibition. Real-time PCR was carried to determine remaining RNA level compared to the starting time point. The trajectory of Pgc1a mRNA was fit into a first order decay curve to derive the RNA half-life. n=4.

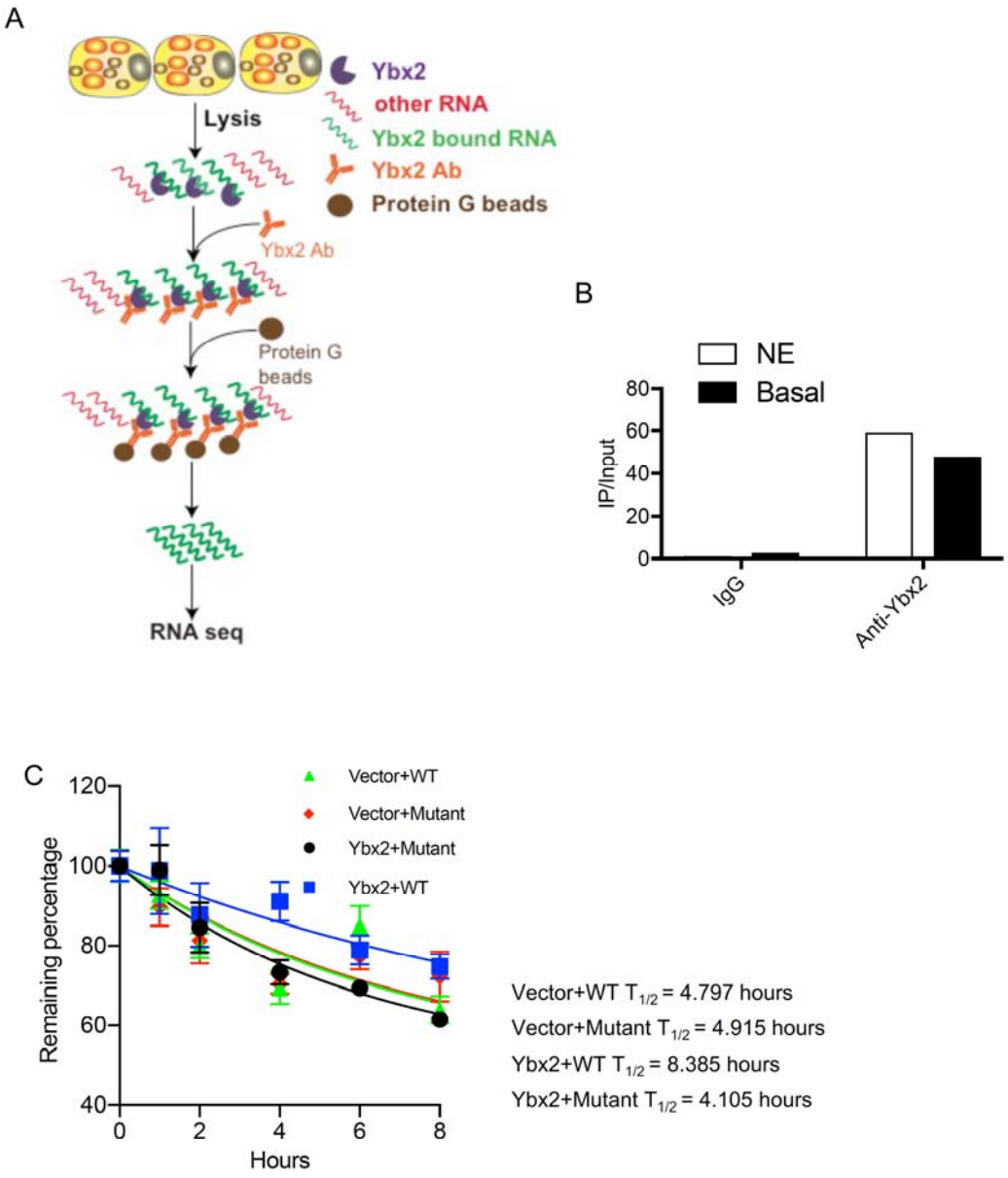

SUPPLEMENTARY DATA

Supplementary Figure S9. (A) WT and KO animals (8-9 weeks old) were housed at 4°C for 6 hours. Skeletal muscle tissues (Gastrocnemius) were harvested for real-time PCR analysis. (B) The OCRs of muscle lysates were measured with Oroboros respirometry. n=6, Error bars are mean ± SEM, *p<0.05, Student's t-test. (C) Western blot to examine the cellular distribution of Ybx2 in BAT nuclear vs. cytosolic lysate.

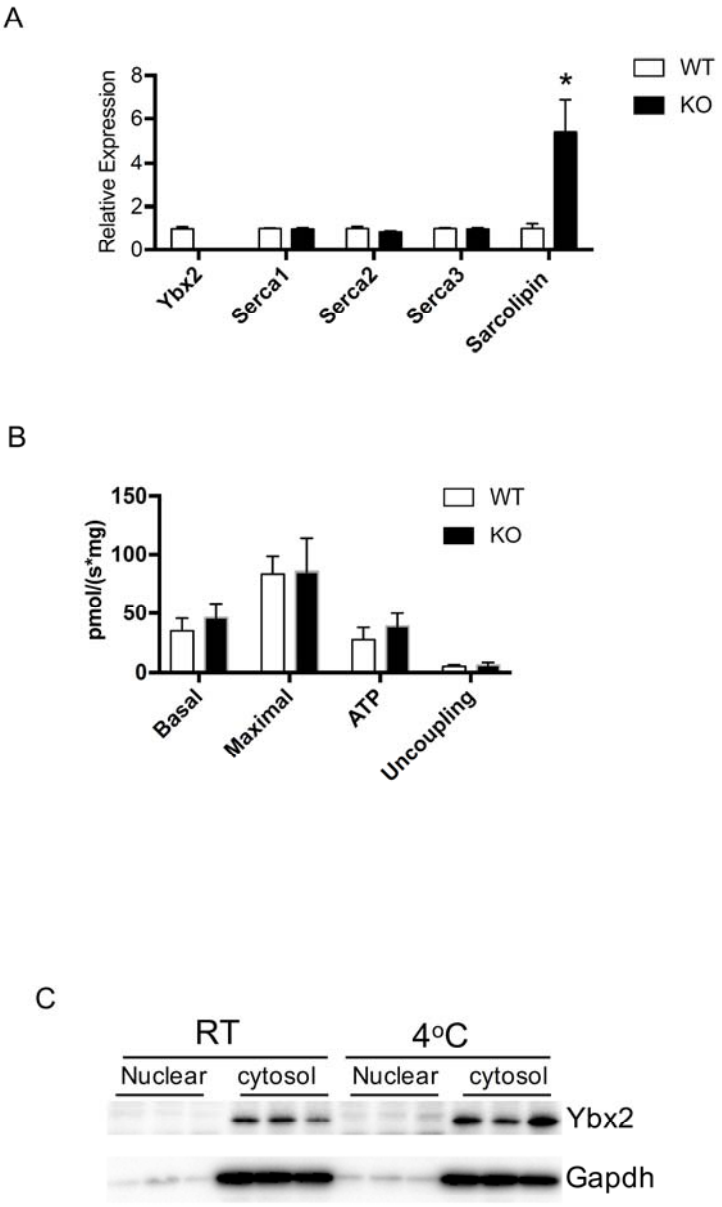

SUPPLEMENTARY DATA

Suppl file1_oligo sequences

Suppl file2_BAT_WT and KO_RNA-seq
https://www.dropbox.com/s/olt27q7d2o2i1jo/Suppl%20file2_BAT_WT%20and%20KO_RNA-seq.xlsx?dl=0

Suppl file3_AdipocyteD5_WT and KO_RNA-seq
https://www.dropbox.com/s/1u4y0p0kk6jjt4c/Suppl%20file3_AdipocyteD5_WT%20and%20KO_RNA-seq.xlsx?dl=0

Suppl file4_RIP-seq and targets
https://www.dropbox.com/s/3s21ch019fi4zqm/Suppl%20file4_RIP-seq%20and%20targets.xlsx?dl=0

Suppl file5_target expression
https://www.dropbox.com/s/0rdd40n630u8zdy/Suppl%20file5_target%20expression.xlsx?dl=0